University of Texas Rio Grande Valley

ScholarWorks @ UTRGV

School of Medicine Publications and Presentations

School of Medicine

2017

Cordycepin induces human lung cancer cell apoptosis by inhibiting nitric oxide mediated ERK/Slug signaling pathway

Jung-Hoo Hwang

Soo Kyung Park

Won Gyo Ko

Seong-Mun Kang

Da Bin Lee

See next page for additional authors

Follow this and additional works at: https://scholarworks.utrgv.edu/som_pub

 Part of the Medicine and Health Sciences Commons

Authors

Jung-Hoo Hwang, Soo Kyung Park, Won Gyo Ko, Seong-Mun Kang, Da Bin Lee, Junho Bang, Byunghun Lee, Byung-Joo Park, Chung-Beum Wee, and Dae Joon Kim

Am J Cancer Res 2017;7(3):417-432
www.ajcr.us /ISSN:2156-6976/ajcr0050713

Original Article

Cordycepin induces human lung cancer cell apoptosis by inhibiting nitric oxide mediated ERK/Slug signaling pathway

Jung Hoo Hwang[1*], Soo Jung Park[2*], Won Gyu Ko[1], Seong-Mun Kang[1], Da Bin Lee[1], Junho Bang[1], Byung-Joo Park[1], Chung-Beum Wee[1], Dae Joon Kim[3], Ik-Soon Jang[4], Jae-Hong Ko[1]

[1]Department of Physiology, Chung-Ang University College of Medicine, Seoul 06974, Republic of Korea; [2]Department of Sasang Constitutional Medicine, Woosuk University, Wanju 55338, Jeonbuk, Republic of Korea; [3]Department of Biomedical Sciences, School of Medicine, University of Texas Rio Grande Valley, Edinburg, TX 78539, USA; [4]Division of Bioconvergence Analysis, Korea Basic Science Institute, Daejeon 305-333, Republic of Korea. [*]Equal contributors.

Received February 13, 2017; Accepted February 16, 2017; Epub March 1, 2017; Published March 15, 2017

Abstract: Nitric oxide (NO) is an important signaling molecule and a component of the inflammatory cascade. Besides, it is also involved in tumorigenesis. Aberrant upregulation and activation of the ERK cascade by NO often leads to tumor cell development. However, the role of ERK inactivation induced by the negative regulation of NO during apoptosis is not completely understood. In this study, treatment of A549 and PC9 human lung adenocarcinoma cell lines with cordycepin led to a reduction in their viability. Analysis of the effect of cordycepin treatment on ERK/Slug signaling activity in the A549 cell line revealed that LPS-induced inflammatory microenvironments could stimulate the expression of TNF-α, CCL5, IL-1β, IL-6, IL-8 and upregulate NO, phospho-ERK (p-ERK), and Slug expression. In addition, constitutive expression of NO was observed. Cordycepin inhibited LPS-induced stimulation of iNOS, NO, p-ERK, and Slug expression. L-NAME, an inhibitor of NOS, inhibited p-ERK and Slug expression. It was also found that cordycepin-mediated inhibition of ERK downregulated Slug, whereas overexpression of ERK led to an upregulation of Slug levels in the cordycepin-treated A549 cells. Inhibition of Slug by siRNA induced Bax and caspase-3, leading to cordycepin-induced apoptosis. Cordycepin-mediated inhibition of ERK led to a reduction in phospho-GSK3β (p-GSK3β) and Slug levels, whereas LiCl, an inhibitor of GSK3β, upregulated p-GSK3β and Slug. Overall, the results obtained indicate that cordycepin inhibits the ERK/Slug signaling pathway through the activation of GSK3β which, in turn, upregulates Bax, leading to apoptosis of the lung cancer cells.

Keywords: Cordycepin, nitric oxide, ERK, slug, lung cancer, apoptosis

Introduction

Nitric oxide (NO) is a ubiquitous, water soluble, free radical gas, playing a central role in a number of physiological as well as pathological processes. Over the past few decades, NO has been shown as a biologically important molecule in carcinogenesis and tumor growth related studies. It modulates different cancer-related events, such as apoptosis, neovascularization of tumors, invasion, metastasis and survival. In some cases, NO or nitric oxide synthase (NOS) levels correlate with tumor growth inhibition and in the others, they are related to tumor cell proliferation, invasion and metastasis [1-3]. Some studies have examined the correlation between inducible NOS (iNOS) and cancer progression and demonstrated an induction of inflammatory response [3]. Lipopolysaccharide (LPS) is known to stimulate immune cells in the tumor microenvironment to generate pro-inflammatory cytokines [4].

Extracellular signal-regulated kinase (ERK) is associated with cancers in humans and plays a crucial role in gene expression, differentiation, proliferation, cell survival, and apoptosis. MEK is a MAPKK (Mitogen-activated protein kinase kinase) that activates MAPK (ERK). The seven human MEKs are involved in four signaling pathways, namely ERK1/2 (MEK1/2), p38 (MEK3/6 and sometimes MEK4), c-Jun N-terminal kinases (JNK) (MEK4/7), and ERK5 (MEK5). The only substrates known so far for

MEK1 and MEK2 are ERK1 and ERK2, respectively. The ERK signaling pathway is a major determinant in controlling diverse cellular processes such as growth, survival, apoptosis, differentiation, and migration [4-7].

Snail family transcriptional repressor 2 (Slug) protein, belonging to the highly conserved Slug/Snail family, is a zinc finger transcriptional repressor. The Slug/Snail protein family is present in a number of species, ranging from *C. elegans* to humans. The protein is upregulated during metastatic lung cancer, breast cancer, and mesothelioma. Recent studies strongly suggest that Slug acts as a potent inducer of cell survival and movement. Besides, suppression of Slug was also found to induce apoptosis [8-12].

Cordycepin (3'-deoxyadenosine), the major bioactive component of *Cordyceps militaris*, has a wide range of biological effects, such as the regulation of immunomodulatory, anti-inflammatory, antibacterial, and antitumor effects. The primary pharmacological activity of *Cordyceps militaris* extracts depends on the main ingredients of the extract. Moreover, cordycepin has been shown to exert a large variety of anti-tumor effects. Some studies have demonstrated that cordycepin induces apoptotic effect through the regulation of MAPK/ERK and Slug signaling pathways [13-15].

In this study, LPS-mediated simulation of inflammatory microenvironment was carried out *in vitro*, which led to increased expression of NO in the lung cancer cell line, A549. This was followed by elucidation of the functional mechanisms underlying the stimulation of ERK/Slug signaling pathway by NO in lung cancer cell lines. Cordycepin prevented the NO-mediated constitutive activation of ERK and Slug transcription factors through the stimulation of GSK3β. It was also established that the consequent activation of the Bax/caspase-3/PARP-pathway leads to cancer cell death.

Materials and methods

Reagents and chemicals

Fetal bovine serum (FBS), 1% (w/v) penicillin-streptomycin, and phosphate-buffered saline (PBS) were procured from Thermo Fischer Scientific™ (Paisley, Scotland, UK). Dulbecco's Modified Eagle's Medium (DMEM), L-NG-nitroarginine methyl ester (L-NAME), LiCl (CAS Number 7447-41-8, 203637 ALDRICH), and LPS (Lipopolysaccharides, L5418) were purchased from Sigma-Aldrich™ (St. Louis, MO, USA). Cordycepin (3'-Deoxyadenosine from *Cordyceps militaris*) was procured from R&D system (R&D Systems, Minneapolis, MN). Annexin-V-FLUOS staining kit was purchased from two different sources, namely Roche Diagnostics GmbH (Mannheim, Germany) and Sigma Chemical Co. Whole cell lysis buffer was procured from iNtRON™ Biotechnology Inc. (Seoul, Korea). The transfection reagent Hilymax and the cell-counting kit-8 were purchased from Dojindo (Dojindo, Japan). Antibodies against phosphorylated ERK (p-ERK), B cell lymphoma-2 (Bcl-2), caspase 3, poly ADP ribose polymerase (PARP-1), GSK3β, p-GSK3β and β-actin were obtained from Cell Signaling (Beverly, MA, USA). Antibodies against ERK, Slug and Bax were procured from Santa Cruz Biotechnology (Dallas, TX, USA).

Cell lines and cell viability assay

The human lung adenocarcinoma cell lines, A549 and PC9, were obtained from the American Type Culture Collection (Rockville, MD, USA). Cells were raised in DMEM medium, supplemented with 10% (v/v) FBS and 1% (w/v) penicillin-streptomycin at 37°C with 5% (v/v) CO_2. The cells (5×10^3/well) were prepared into a 96-well plate. After 24 h of incubation, the cells were treated cordycepin for 48 h, after which the cell viability assays were performed. Briefly, at the end of the treatment, 10 μL of the cell-counting kit-8 solution (Dojindo, Japan) was added to the cells and incubated for 1 h at 36°C. Cell viability was determined by measuring the absorbance at 450 nm using a microplate reader (Sunrise, Tecan, Switzerland). The assays were performed in triplicates. Appropriate dose of cordycepin required for treatment of A549 cell line was determined by evaluating the cytotoxicity of cordycepin for 48 h, followed by generation of micrographs of the treated cells.

Cell cycle analysis by PI-Annexin-V staining

Effect of cordycepin on apoptosis was analyzed using Annexin-V-FLUOS staining kit (Roche Diagnostics) and observing the Annexin-V/propidium iodide (PI) staining patterns. The cells were treated with cordycepin for 48 h, after which they were scraped off and washed twice with phosphate buffered saline (PBS). The cell

suspension was centrifuged at 2000 rpm for 2 min and the pellet obtained was incubated with 0.2 mg/mL Annexin-V FLUOS and 1.4 mg/mL propidium iodide for 15 min at room temperature. This was followed by fluorescence measurements in an Image Cytometer (NUCLEOCOUNTER® NC-3000™, Chemometec, Copenhagen, Denmark) at an excitation wavelength of 488 nm, with a 530/30 nm bandpass filter to detect Annexin-V and a 670-nm high-pass filter to detect propidium iodide (PI).

Microarray analysis

Transcriptional profiling of the cordycepin-treated A549 cancer cells was carried out using a human twin 44K cDNA chip. Total RNA was extracted from vehicle or 60 μg/mL cordycepin-treated A549 cancer cells. This was followed by synthesis of cDNA probes using 50 mg RNA in the presence of aminoallyl dUTP by reverse transcription. The cDNA was coupled with Cy3 (vehicle) or Cy5 dye (cordycepin-treated). Genes were considered to be differentially expressed when after a significance analysis of the microarray (SAM), the global M value, and log2 (R/G) exceeded |1.0| (twofold), with a p-value < 0.05. A student's t-test was applied to assess the statistical significance of the differential expression of genes after cordycepin treatment. In order to analyze the biological significance of the changes, the array data was categorized into specific gene groups.

Ontology-related network analysis

To study the biological role of ontology-related regulated genes and proteins through their interaction networks, a bioinformatic network analysis was conducted using the ingenuity pathway analysis (IPA, http://www.ingenuity.com). IPA identifies a gene interaction network based on the regularly-updated "Ingenuity Pathways Knowledge-base". The updatable database was retrieved from biological literature. Network generation, aimed at the production of highly-connected networks, was optimized using the input expression profiles whenever possible.

Western blot analysis

Expression profiles of cordycepin-treated apoptosis-related signaling proteins were examined using western blotting. Denatured proteins (25 μg) was resolved on 12% polyacrylamide gel and transferred onto a nitrocellulose membrane. The nitrocellulose membrane was stained with Ponceau S to position the proteins. The blotted membrane was blocked for 1 h with 5% (w/v) skimmed milk in TTBS (Tween-20 and Tris-buffered saline), followed by incubation with a dilution of primary antibodies, ERK (1:500), p-ERK (1:200), Bcl-2 (1:500), Slug (1:500), caspase-3 (1:200), Bax (1:1000), PARP-1 (1:1000), GSK3β, p-GSK3β and β-actin (1:2000), at room temperature for 2 h or, alternatively, at 4°C overnight. After incubation, the membrane was washed thrice with 0.1% (v/v) Tween-20 in TBS for 5 min, followed by incubation with horseradish-peroxidase (HRP)-conjugated goat anti-mouse IgG or HRP-conjugated rabbit anti-goat IgG with a 1:2000 dilution in TBS containing 5% (w/v) skimmed milk at room temperature for 1 h. The membranes were then washed thrice for 5 min with TTBS, followed by visualization using an enhanced chemiluminescence system (Thermo Scientific, San Jose, CA, USA). The bands were visualized on a ChemiDoc MP system (Bio-Rad, Hercules, CA, USA). Densitometric measurements of bands were performed using Image J software. Expression levels of proteins were quantitatively analyzed through comparisons with actin as an internal control.

Biochemical analysis

For overexpression of ERK, lentivirus carrying red fluorescent protein (RFP)-conjugated full-length ERK1 (Lenti H1.4-ERK1/RFP; Bioneer Corp., Daejeon, Korea) was used. Small interfering RNAs (siRNAs) were purchased from Cell signaling and ST Pharm (Seoul, Korea). The nucleotide sequence for Slug (GenBank AF084243.1) siRNAs was 5'-AAG ATC TGA ACA CAA GTG ACT-3'. A549 cells were seeded (2×10^5 cells/6-well plates) on a microtiter plate. After incubation, the cells were supplied with growth medium containing 10% FBS and were harvested after 48 h for further assays. The transfection of siRNA into A549 cells was performed using lipofectamine RNAiMAX reagent (Invitrogen, Carlsbad, CA, USA), according to manufacturer's instructions. After transfection, the cells were treated with cordycepin (60 μg/mL) for 48 h.

Determination of NO levels

NO levels were determined colorimetrically using a NO detection kit based on the Griess

method, which indirectly measures the concentration of NO by determining nitrite (NO_2^-) concentrations. For the assay, 100 µL samples were collected and added to wells in triplicates. This was followed by addition of 50 µL of N1 buffer to the wells and incubation at room temperature (RT) for 10 min. Afterwards, N2 buffer (50 µL) was added and the final reaction was carried out for 10 min at RT. Absorbance between 520-560 nm was measured using an ELISA reader (Multiskan EX, Thermo Lab systems, Beverly, MA, USA). Nitrite levels were determined using a standard curve.

Measurements of cytokines

The levels of five different cytokines and chemokines interleukin 1 beta (IL-1β), IL-6, IL-8, chemokine C-C motif ligand 5 (CCL5/RANTES), and tumor necrosis factor-α (TNF-α) were measured in the growth medium supernatants of A549 cells using a bead-based multianalyte bead immunoassay (Invitrogen Cytokine human 25-plex panel, Cat No. LHC0009), according to the manufacturer's protocol. Briefly, diluted (1:2) culture supernatants were incubated with internally dyed polystyrene beads coated with specific antibodies directed against one of the cytokines. Proteins present in the culture supernatants bound to the antibody-coated beads during a 2 h incubation period, after which the beads were washed extensively. Biotinylated detector antibodies directed against specific proteins were added to the beads, where they bind to proteins derived from culture supernatants. After washing, streptavidin-conjugated R-phycoerythrin was added to the bead-culture supernatant derived protein-detector antibody complexes. This was followed by washing of the unbound streptavidin-conjugated R-phycoerythrin, and analysis of the bead complexes using Luminex Detection system (Luminex® 200™ System, Thermo). Cytokine and chemokine concentrations in culture supernatants were extrapolated based on a standard curve generated using manufacturer-supplied standards of each cytokine analyte.

Migration assay

The migration assay was conducted on control and LPS, L-NAME, and cordycepin treated A549 cells. The cells were seeded onto a 24-well plate. The monolayer was then scraped using a pipette tip to create a wound. The cells were treated with cordycepin (100 µg/mL) for 48 h. The plates were visualized using the TissueFAXS system (TissueGontics, Vienna, Austria). Cell migration was analyzed in terms of the "healed" area migrated cells using the HistoQuest software (TissueGnostics, Vienna, Austria). The samples were analyzed using Zeiss AxioImagerZ1 microscope system fitted with a charge-coupled device camera and the TissueFAXS™ automated acquisition system (TissueGnostics, Vienna, Austria). The percentages of antibody-positive and stemness marker-positive tumors were calculated and depicted as scatter graphs. Images were digitalized and protein expression was quantified. Statistical flow analysis was performed using the HistoQuestTM software (TissueGnostics).

Immunofluorescence microscopy

A549 cells were seeded at a density of 4×10^4 cells/well on a coverslip in a 12-well plate. The cells were pre-treated with cordycepin, LiCl, and LPS with si-ERK for 24 h, followed by washing with 250 µM PBS (pH 7.5) twice and fixation with 4% (v/v) formaldehyde for 15 min. The fixed cells were permeabilized using 0.1% (v/v) Triton X-100 for 15 min and then incubated with 3% (w/v) bovine serum albumin (BSA) for 1 h to prevent nonspecific binding. Thereafter, the cells were incubated with the primary antibody (Slug monoclonal purified mouse IgG1 diluted to 1:100 in 3% (w/v) BSA) overnight at 4°C, followed by 1 h incubation with the secondary antibody [fluorescein isothiocyanate-anti-mouse antibody diluted to 1:200 in 3% (w/v) BSA (Invitrogen Life Technologies, Carlsbad, CA, USA)] in dark. The coverslips were washed with PBS and mounted with mounting solution for observation. Images were acquired using an LSM 710 laser-scanning confocal microscope (Carl Zeiss, Jena, Germany) at 488 nm Ar laser. Image data were analyzed with ZEN 2009 Light Edition software.

Statistical analyses

GraphPad Prism software (GraphPad, San Diego, CA, USA) was used for the statistical analyses. The student's t-test was used to assess the statistical difference between control and the cordycepin-treated groups. *P* values less than 0.05 were considered as statistically significant.

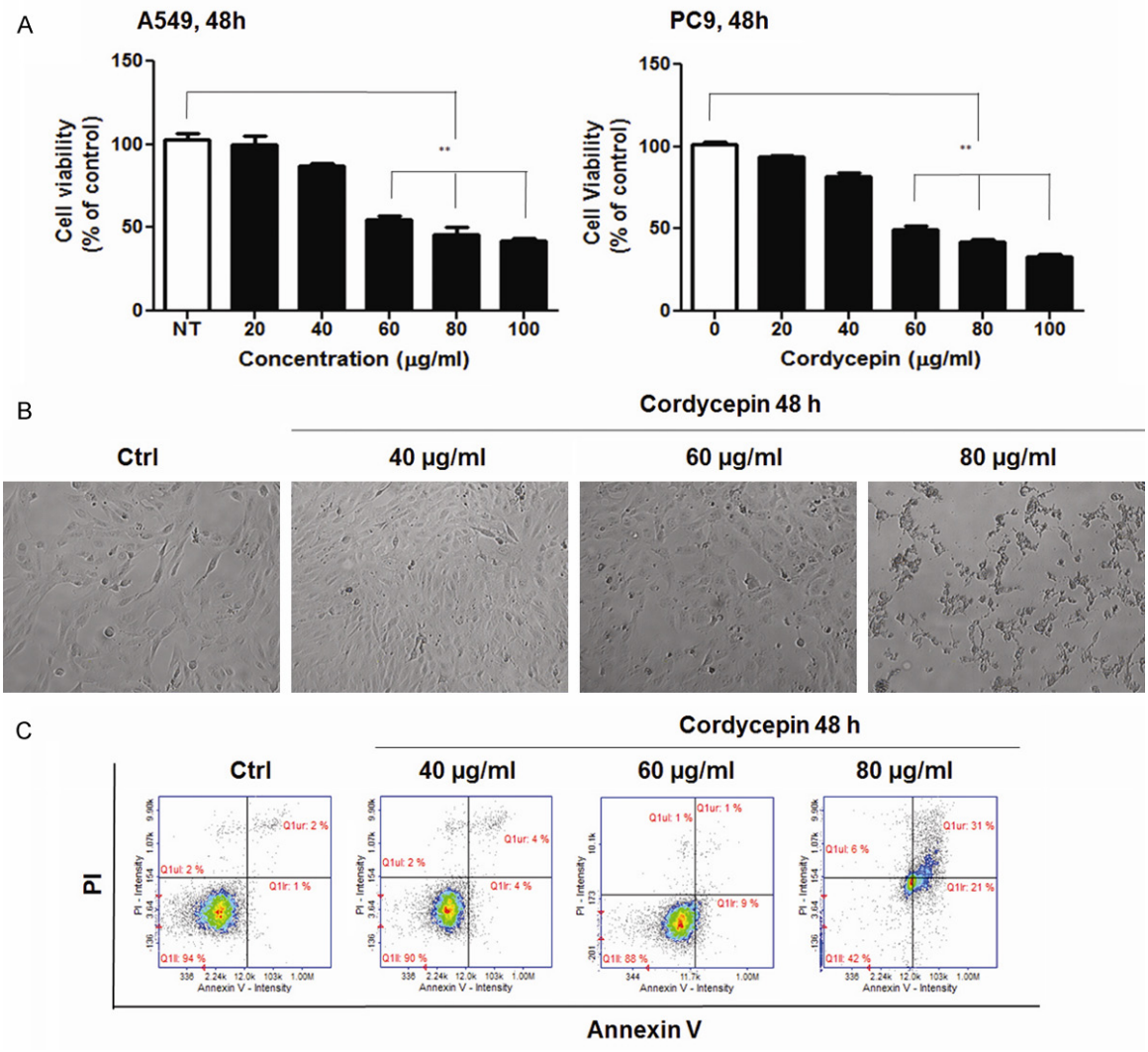

Figure 1. Viability and morphology of lung cancer cells after treatment with cordycepin. (A) Inhibition of the growth of A549 and PC9 lung adenocarcinoma cells by cordycepin. Lung cancer cells were exposed to 0, 20, 40, 60, and 100 μg/mL cordycepin for 48 h. The data are presented as mean ± standard deviation from triplicate experiments. Statistical significance was considered as $^{**}P < 0.01$ vs. Non-treat control (B) Microscopic images of A549 cells treated with cordycepin for 48 h. Magnification 400 ×. (C) Analysis of apoptosis of A549 cells exposed to cordycepin.

Results

Inhibition of growth in lung cancer cells by cordycepin

Cordycepin was used directly to pretreat A549 and PC9 lung adenocarcinoma cells to examine its effect on cell viability. Treatment with cordycepin gradually decreased the growth of both the cell lines during 48 h of incubation (**Figure 1**). For the quantitative determination of 50% inhibitory concentration (IC_{50}) values, cordycepin was administered at 0, 20, 40, 60, 80, and 100 μg/mL for 48 h. At 60 μg/mL, cordycepin inhibited approximately 50% of the A549 and PC9 cell populations. This value was, therefore, taken as the IC_{50} of cordycepin. The cell morphology of A549 cell lines were observed in order to assess the effect of cordycepin treatment on apoptosis (**Figure 1B**). Light microscopy revealed a change in the morphology of A549 cells after treatment with cordycepin. The cells began to detach from the surface of the culture plate and appeared buoyant. A change in shape from round to pointed pole-like structure was also observed. These morphological changes preceded apoptosis. The apoptotic effect of cordycepin on A549 lung

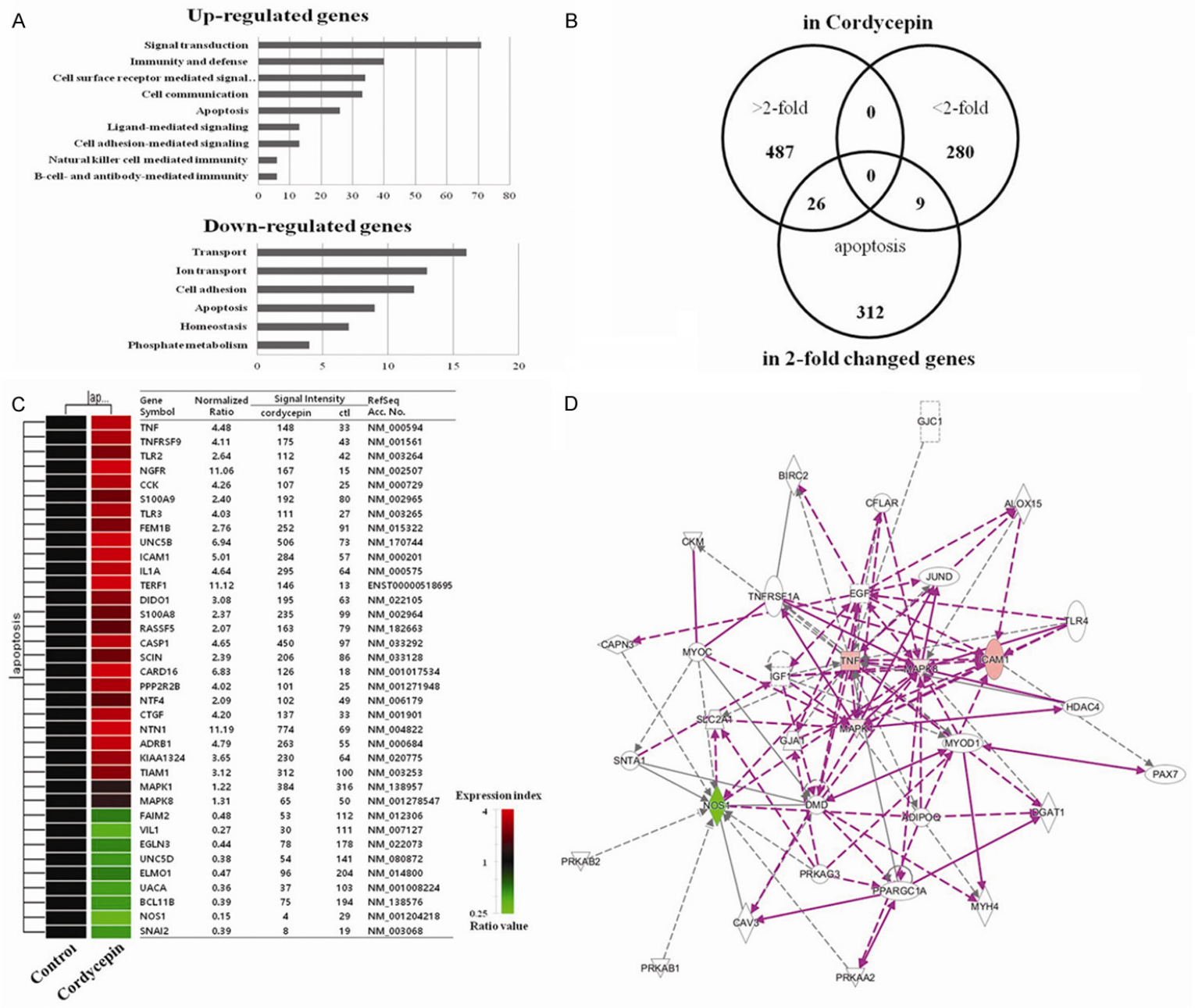

Gene Symbol	Normalized Ratio	Signal Intensity cordycepin	Signal Intensity ctl	RefSeq Acc. No.
TNF	4.48	148	33	NM_000594
TNFRSF9	4.11	175	43	NM_001561
TLR2	2.64	112	42	NM_003264
NGFR	11.06	167	15	NM_002507
CCK	4.26	107	25	NM_000729
S100A9	2.40	192	80	NM_002965
TLR3	4.03	111	27	NM_003265
FEM1B	2.76	252	91	NM_015322
UNC5B	6.94	506	73	NM_170744
ICAM1	5.01	284	57	NM_000201
IL1A	4.64	295	64	NM_000575
TERF1	11.12	146	13	ENST00000518695
DIDO1	3.08	195	63	NM_022105
S100A8	2.37	235	99	NM_002964
RASSF5	2.07	163	79	NM_182663
CASP1	4.65	450	97	NM_033292
SCIN	2.39	206	86	NM_033128
CARD16	6.83	126	18	NM_001017534
PPP2R2B	4.02	101	25	NM_001271948
NTF4	2.09	102	49	NM_006179
CTGF	4.20	137	33	NM_001901
NTN1	11.19	774	69	NM_004822
ADRB1	4.79	263	55	NM_000684
KIAA1324	3.65	230	64	NM_020775
TIAM1	3.12	312	100	NM_003253
MAPK1	1.22	384	316	NM_138957
MAPK8	1.31	65	50	NM_001278547
FAIM2	0.48	53	112	NM_012306
VIL1	0.27	30	111	NM_007127
EGLN3	0.44	78	178	NM_022073
UNC5D	0.38	54	141	NM_080872
ELMO1	0.47	96	204	NM_014800
UACA	0.36	37	103	NM_001008224
BCL11B	0.39	75	194	NM_138576
NOS1	0.15	4	29	NM_001204218
SNAI2	0.39	8	19	NM_003068

Figure 2. Gene expression and signaling network analysis of ERK-Slug signaling-related genes. (A) Results of gene ontology analysis by using microarray approaches. Gene lists corresponding to 2-fold up- and downregulation in cordycepin-treated A549 cells for 48 h (B) Venn diagram of hierarchical clustering revealed genes that were altered more than 2-folds upon apoptosis in response to cordycepin. (C) 35 gene lists (> 2-fold, < 2-fold, and apoptosis-related genes) are shown and are intersected individually by using Venn diagram. The red and green colors represent more than two fold up- and downregulated genes, respectively. (D) Signaling network of the apoptosis-related genes in response to cordycepin. Nodes colored by using a Qiagen IPA (red: upregulated genes, green: downregulated genes).

cancer cells was analyzed using Annexin V and PI staining by flow cytometry (**Figure 1C**). The assay was performed to assess the induction of apoptosis of cancer cells by cordycepin. For the evaluation of apoptosis, the relative proportion of non-viable cells was quantitatively measured as the cells entered early stage of apoptosis (Annexin stained, non-disrupted cells) or as the cells entered late stages of apoptosis (disrupted or lysed cells). The flow cytometric analyses of both the A549 cells was performed and was compared before and after treatment with 40, 60, and 80 μg/mL cordycepin for 48 h. Many Annexin V-stained viable A549 cells shifted to the late apoptotic stage (2% to 31%). This suggests that cordycepin induced the apoptotic process differently in lung cells.

Effect of cordycepin on gene expression profiles in lung cancer cell

To identify potential genes involved in the anticancer activity of cordycepin, microarray analysis was performed for A549 cancer cells after treatment with cordycepin. Out of a total of 62,442 unique genes (using Agilent's Human GE 8x60K Microarray) analyzed, 28,812 genes were expressed cells treated with 60 μg/mL of cordycepin. Among these, 2,439 and 1,447 genes were up- and downregulated, respectively, by treatment with 60 μg/mL cordycepin compared to the untreated control after 48 h. The genes that were up- or downregulated by more than 2-folds were significantly handled in the data mining categories. Biologically relevant features were constructed using the Database for Annotation, Visualization, and Integrated Discovery (DAVID) tools (http://david.abcc.ncifcrf.gov/). Gene lists corresponding to 2-fold up- or downregulation in the cordycepin-induced lung cancer cells were uploaded to DAVID for Gene Ontology analysis (**Figure 2A**). The upregulated genes were the ones involved in signal transduction, immunity and defense, cell surface receptor mediated signaling, cell communication, apoptosis, ligand-mediated signaling, cell adhesion-mediated signaling, natural killer cell mediated immunity, B-cell and antibody-mediated immunity. Downregulated genes included those involved in transport, ion transport, cell adhesion, apoptosis, homeostasis, and phosphate metabolism. To compare the results obtained upon cordycepin treatment with potential genes that are involved in apoptosis, we identified candidate 35 genes using the GeneCards database (http://www.genecards.org/) (**Figure 2B**). The intersection obtained by hierarchical clustering is presented along with the 35 gene lists in **Figure 2C**. The signal network of apoptotic genes in response to cordycepin is shown in **Figure 2D**. The hub genes are MAPKs, NOS, ICAM1 (Intercellular Adhesion Molecule 1), and TNF (tumor necrosis factor).

ERK-Slug signaling linked apoptosis by cordycepin in A549 lung cancer cell

In various cell line models, apoptotic cell death is induced by the serial activation of caspases. To investigate whether cordycepin affects caspase activation to induce apoptosis, the expression profiles of p-ERK, ERK, Slug, Bcl-2, Bax, caspase-3, cleaved caspase-3, PARP-1, and cleaved PARP1 were observed by western blot analysis of the A549 cell line (**Figure 3**). The expression level of pro-apoptosis protein Bax remained unchanged after the treatment with 60 μg/mL cordycepin. On the other hand, expression level of anti-apoptosis protein Bcl-2 was decreased and the expression of the active form of cleaved caspase-3 and cleaved PARP-1 were significantly increased after treatment with cordycepin. These results corroborated the flow cytometric analysis (**Figure 1C**), suggesting that A549 cells were sensitive to cordycepin treatment and ultimately underwent apoptosis. Based on these data, effect of cordycepin on the inhibition of ERK and Slug pathways was assessed. The expression of p-ERK and Slug were clearly downregulated in the presence of cordycepin.

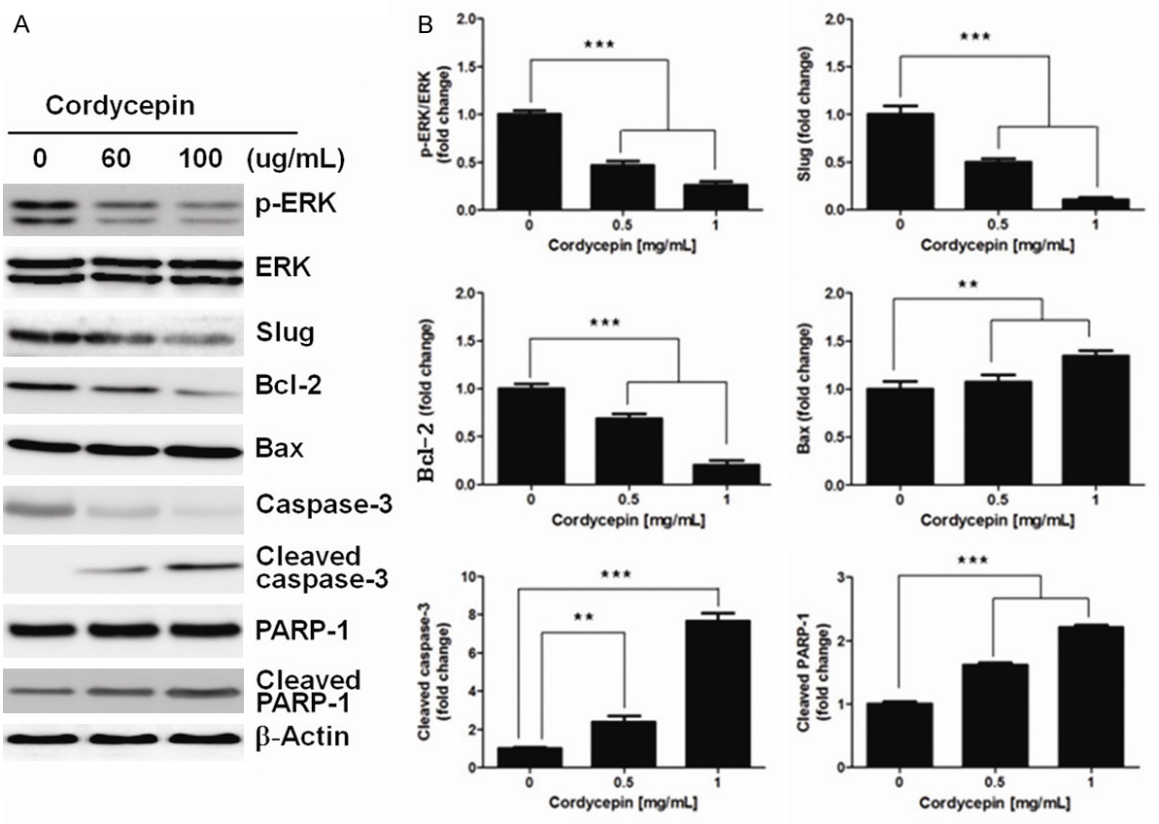

Figure 3. Protein expression post cordycepin treatment in lung cancer A549 cells. (A) Western blots showing the expression of p-ERK, ERK, Slug, Bcl-2, Bax, caspase-3, cleaved caspase-3, PARP-1, and cleaved PARP-1, and (B) relative band intensities in response to treatment with 0, 60 and 100 μg/ml of cordycepin in A549 cells. Data are expressed as means ± SD, $^{**}P < 0.01$, $^{***}P < 0.001$.

Cordycepin-induced reduction in NO production by inhibition of NOS and LPS-induced cytokine expression

To verify whether the inhibition of NO production by cordycepin was the mechanism underlying apoptosis, the levels of NO in the cell supernatants of various treatment groups were analyzed (**Figure 4A**). L-NAME is a well-known inhibitor of NOS and, therefore, inhibits NO production. A549 cells were treated with L-NAME (500 μM) for 24 h, leading to the inhibition of NO production, as compared to the non-L-NAME-treated control cells. Further, the cells were treated with L-NAME along with an excess of LPS (10 μg/mL) for 24 h. Presence of LPS blocked the inhibition of NO production by L-NAME. An increase in NO concentration was observed of the cells as compared to the untreated control. These data indicate that endogenous NO plays a role in promoting cell proliferation. The effect of LPS on the cordycepin-induced inhibition of NO production was observed by treatment of A549 cells with cordycepin (60 μg/mL) for 24 h. In the absence of LPS, production of NO was inhibited. Whereas, in the presence of LPS (10 μg/ml), its production was stimulated. Following this, levels of NOS were assessed in the cordycepin-treated cells. Western blot analysis revealed that treatment with cordycepin resulted in the inhibition of iNOS expression in LPS-stimulated A549 cells in a concentration-dependent manner (**Figure 4B**, **4C**). Cancer cells secrete a number of cytokines, which mediate their immune modulatory functions, and affect carcinogenesis, cancer cell proliferation, and metastasis. To investigate the correlation with NO and cytokines in the inflammatory response, levels of TNF-α, IL-1β, IL-6, IL-8, and CCL5 were detected in A549 cells after treatment with LPS (10 μg/ml) for 24 hours (**Figure 4D**). The results obtained demonstrate that LPS mediates the upregulation in the expression and

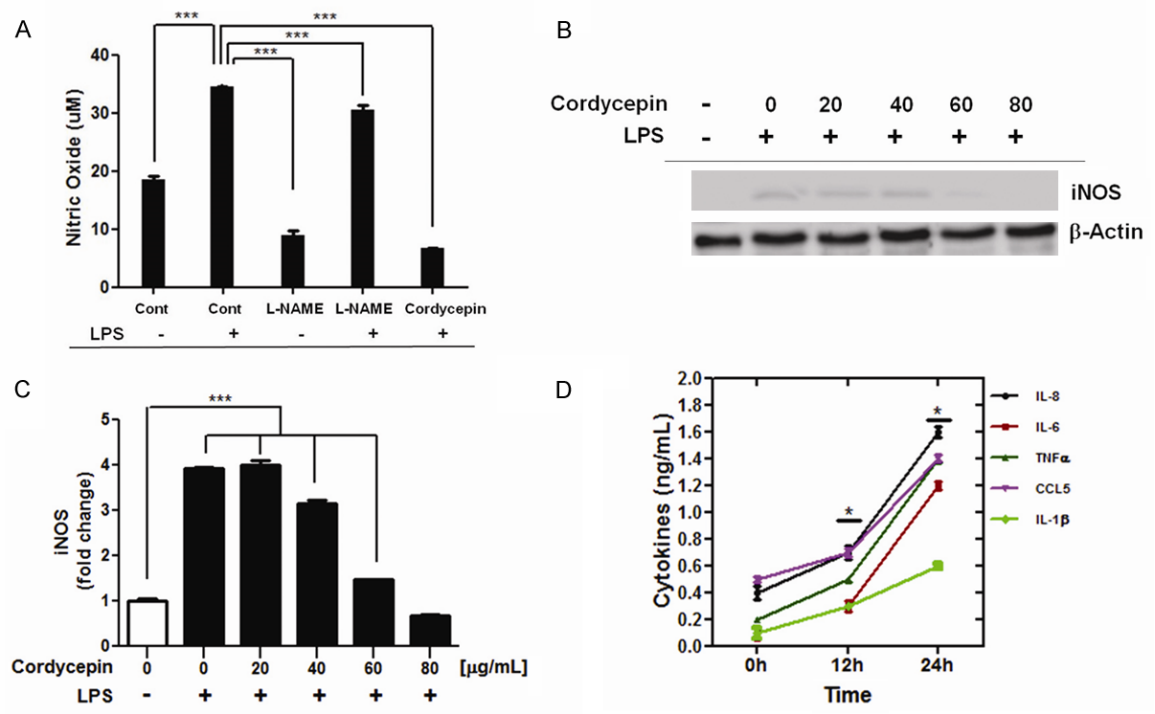

Figure 4. Effect of cordycepin on LPS-induced NO production and iNOS protein expression. (A) Effect of cordycepin on NO production in LPS-stimulated A549 cells. Each column represents the mean ± SD of three independent experiments. ***$P < 0.001$. (B) Effect of cordycepin on LPS-induced iNOS protein expression, and (C) relative band intensities of iNOS. (D) Effect of LPS on release of cytokines and chemokines in A549 cells. At the indicated time points, cell supernatants were harvested and release of IL-1β, IL-6, IL-8, CCL5, and TNF-α was quantified by Human Cytokine Twenty-Five-Plex. *Represents significantly different values from controls.

secretion of cytokines and chemokines, such as TNF-α, CCL5, IL-1β, IL-6, and IL-8.

Inhibition of NO mediated ERK and Slug activation by cordycepin

Reduction in the levels of NO by L-NAME or cordycepin resulted in a decrease in ERK phosphorylation, whereas the increase in the levels of NO by LPS led to activation of ERK (**Figure 5A** and **5B**). A significant reduction in LPS-induced ERK phosphorylation was observed in the presence of cordycepin, suggesting that it mediates the inhibition of ERK by downregulating the production of NO. A549 cells were also treated with the specific NOS inhibitor L-NAME (500 μM) for 6 h, which resulted in the decrease in the basal concentration of p-ERK and Slug in a dose dependent manner (**Figure 5C** and **5D**). To evaluate the potential biological relevance of cordycepin, the effect of NO on the migration of A549 tumor cells (**Figure 5E**) was assessed by a wound-healing assay. Treatment of the cells with L-NAME (500 μM) for 24 h resulted in the inhibition of cell migration compared to non-L-NAME-treated control cells. Further, the cells were treated with L-NAME in the presence of excess amount of LPS for 24 h. Presence of LPS resulted in an increase in cell migration as compared to the cells treated with L-NAME alone. These data indicate that NO plays a crucial role in promoting the migratory behavior of these cells. Thereafter, the effect of LPS on the cordycepin-induced inhibition of migration was analyzed. Treatment of A549 cells with cordycepin (60 μg/mL) in the presence of an excess amount of LPS (10 μg/ml) for 48 h recovered cell migration and stimulated NO production, further suggesting that the inhibition of cell migration by cordycepin is mediated by inhibition of ERK and Slug activation mediated by NO.

Cordycepin downregulates ERK-Slug signaling by inhibiting NO to induce Bax activation

To further investigate if ERK is functionally linked to Slug signaling, the effect of cordyce-

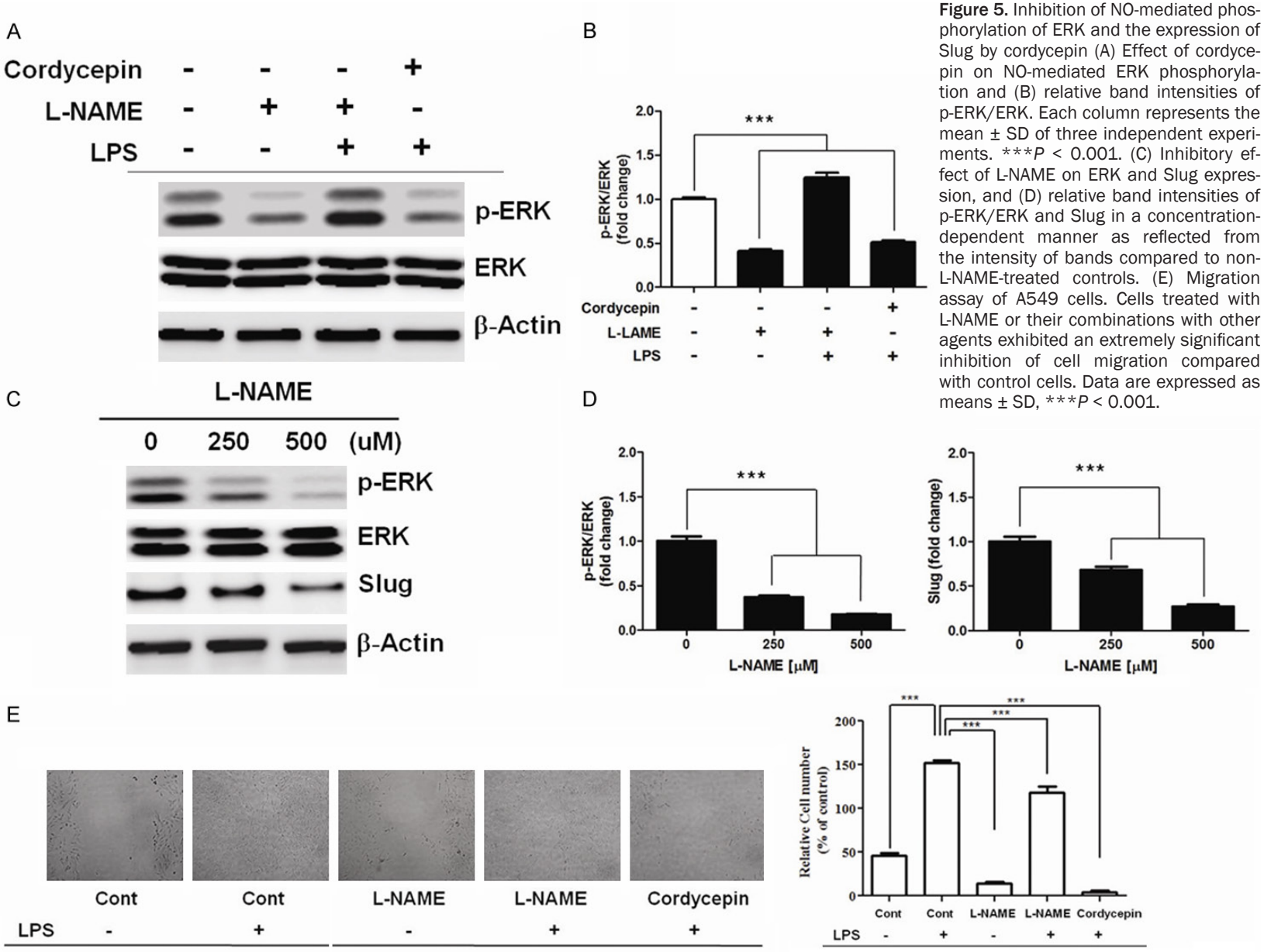

Figure 5. Inhibition of NO-mediated phosphorylation of ERK and the expression of Slug by cordycepin (A) Effect of cordycepin on NO-mediated ERK phosphorylation and (B) relative band intensities of p-ERK/ERK. Each column represents the mean ± SD of three independent experiments. ***$P < 0.001$. (C) Inhibitory effect of L-NAME on ERK and Slug expression, and (D) relative band intensities of p-ERK/ERK and Slug in a concentration-dependent manner as reflected from the intensity of bands compared to non-L-NAME-treated controls. (E) Migration assay of A549 cells. Cells treated with L-NAME or their combinations with other agents exhibited an extremely significant inhibition of cell migration compared with control cells. Data are expressed as means ± SD, ***$P < 0.001$.

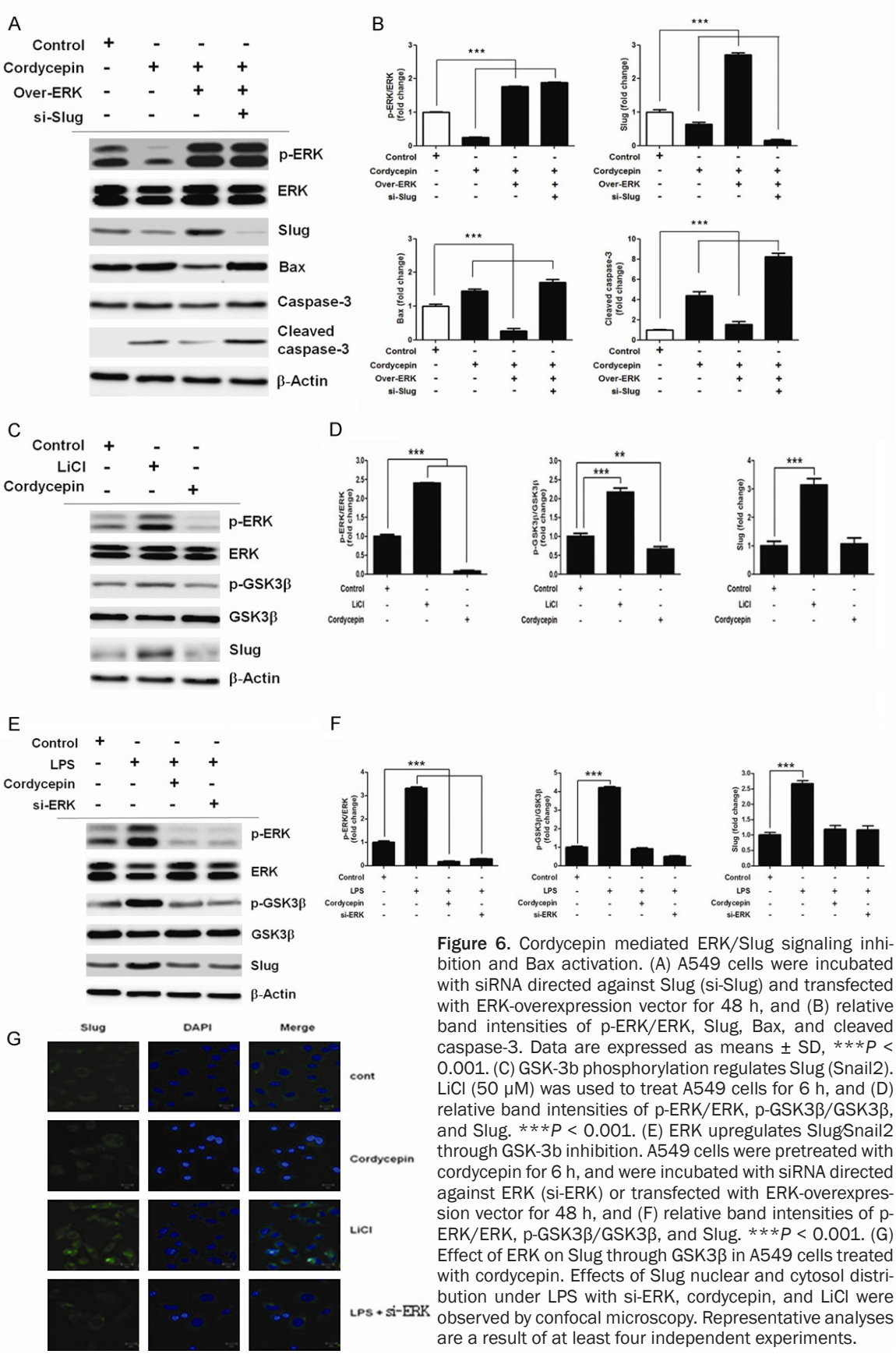

Figure 6. Cordycepin mediated ERK/Slug signaling inhibition and Bax activation. (A) A549 cells were incubated with siRNA directed against Slug (si-Slug) and transfected with ERK-overexpression vector for 48 h, and (B) relative band intensities of p-ERK/ERK, Slug, Bax, and cleaved caspase-3. Data are expressed as means ± SD, ***P < 0.001. (C) GSK-3b phosphorylation regulates Slug (Snail2). LiCl (50 μM) was used to treat A549 cells for 6 h, and (D) relative band intensities of p-ERK/ERK, p-GSK3β/GSK3β, and Slug. ***P < 0.001. (E) ERK upregulates SlugSnail2 through GSK-3b inhibition. A549 cells were pretreated with cordycepin for 6 h, and were incubated with siRNA directed against ERK (si-ERK) or transfected with ERK-overexpression vector for 48 h, and (F) relative band intensities of p-ERK/ERK, p-GSK3β/GSK3β, and Slug. ***P < 0.001. (G) Effect of ERK on Slug through GSK3β in A549 cells treated with cordycepin. Effects of Slug nuclear and cytosol distribution under LPS with si-ERK, cordycepin, and LiCl were observed by confocal microscopy. Representative analyses are a result of at least four independent experiments.

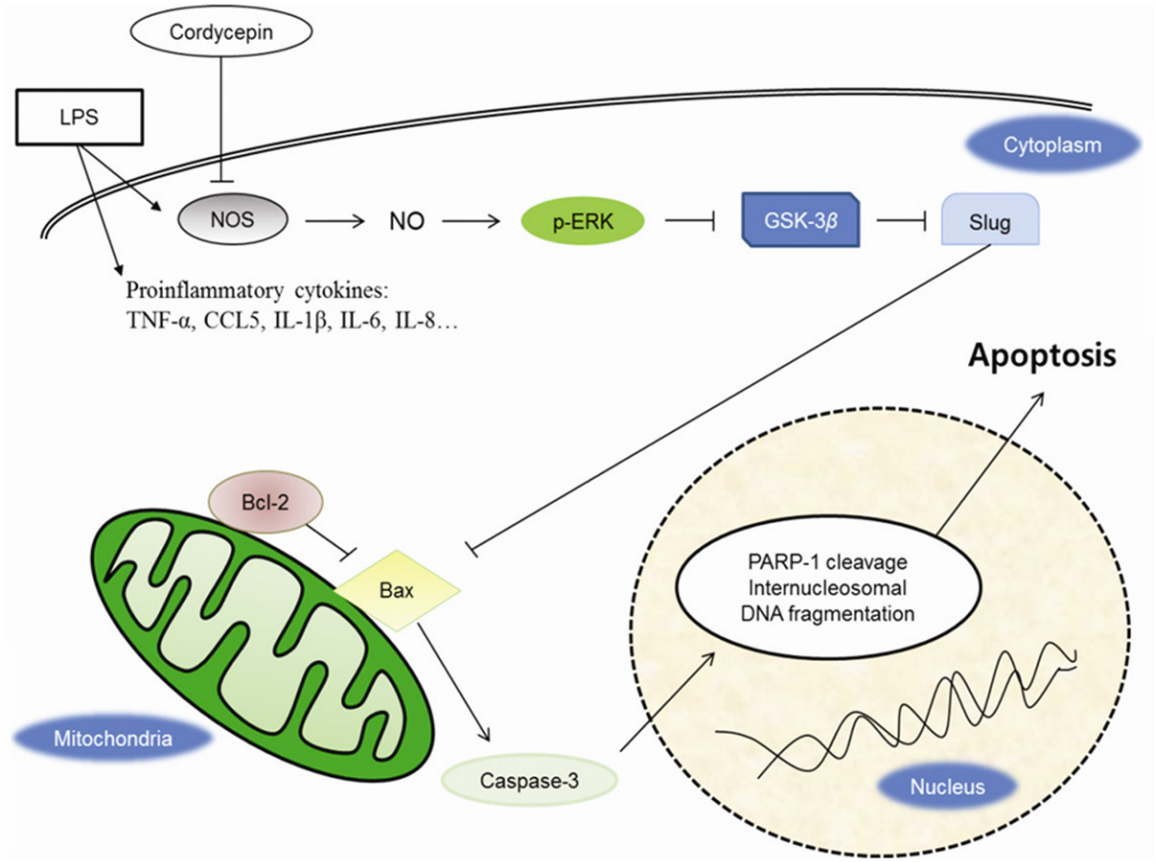

Figure 7. Schematic diagram showing the mechanisms of action of cordycepin based on the findings of this study. LPS-induced inflammatory microenvironment could stimulate the expression of TNF-α, CCL5, IL-1b, IL-6, IL-8 and upregulate p-ERK and Slug. Cordycepin mediates Bax-induced apoptotic regulation of ERK/Slug through GSK3β activation by downregulating NO production.

pin on ERK-Slug signaling was assessed (**Figure 6**). Downregulation of NO signaling was obtained upon cordycepin treatment. Immunoblots confirmed the reduction in ERK and Slug expression in A549 cell line. A loss-of-function analysis using ERK knockdown by cordycepin was performed. Cordycepin led to attenuation of p-ERK and Slug expression, whereas ERK overexpression upregulated p-ERK and Slug in cordycepin-treated A549 cells. siRNA-mediated Slug inhibition enhanced the activation of Bax and caspase-3 (**Figure 6A**, **6B**), indicating that cordycepin-mediated inactivation of ERK downregulated Slug expression, leading to upregulation of Bax. In order to elucidate how the upregulation of ERK enhances Slug activation, a comprehensive immunoblotting analysis of various signaling pathways in A549 cells was performed. As a result, several alterations were identified in the ERK/Slug signaling pathway (**Figure 6**). The presence of GSK3β inhibitor, LiCl (50 μM), alone increased the levels of p-GSK3β and Slug (**Figure 6C**, **6D**). On the other hand, cordycepin mediated inhibition of ERK in A549 cells treated with LPS resulted in decreased levels of p-GSK3β and Slug. Besides, the silencing of ERK alone also resulted in decreased p-GSK3β and Slug levels (**Figure 6E**, **6F**). Consistent with this finding, nuclear translocation of Slug was inhibited upon treatment with cordycepin alone and LPS with si-ERK, whereas increase in both cytosolic and nuclear Slug under LiCl were observed by confocal microscopy (**Figure 6G**). These results indicate that ERK inhibition mediated by cordycepin downregulates the expression of Slug through the activation of GSK3β.

Overall, these results suggest that cordycepin-mediated inhibition of ERK downregulates Slug signaling through the activation of GSK3β by inhibiting NO, which upregulates Bax, and con-

sequently, induces apoptosis in the lung cancer cell lines (**Figure 7**).

Discussion

Cordycepin possesses many important pharmacological properties, including inhibition of inflammation, platelet aggregation, mRNA polyadenylation, and immunological stimulation. In addition, it has remarkable anti-tumor effects, such as cell growth inhibition, induction of apoptosis, and suppression of cell migration and invasiveness [13, 16, 17]. The present study demonstrated that treatment of A549 lung cancer cells with 60 μg/mL cordycepin reduced their viability and led to a significant growth reduction (**Figure 1A**). Moreover, treatment with 60 μg/mL cordycepin altered the cell morphology of A549 cell line, as compared to the untreated control and 40 μg/mL cordycepin-treated cells (**Figure 1B**, **1C**). Annexin V/PI staining of the cells using FACS demonstrated that cordycepin could induce pro-apoptosis. Treatment with cordycepin at 60 μg/mL, but not 40 μg/mL, induced the transformation of cells from normal (untreated group: 91.0% normal, 4.0% early apoptotic, and 3% late apoptotic) to apoptotic state (65.0% normal, 26.0% early apoptotic, and 8.0% late apoptotic) (**Figure 1C**). These results suggest that cordycepin exhibits anti-lung cancer activity by promoting pro-apoptosis.

Analysis of cordycepin-mediated alteration of gene expression levels in lung cancer cells was performed using microarray approach. Clustering of the microarray data identified groups of genes that were differentially regulated upon treatment of the A549 cells with 60 μg/mL of cordycepin. GO categories of genes revealed the genes whose expression changed by at least 2-folds (**Figure 2A**). Among these, 26 upregulated and 9 downregulated genes were involved in apoptosis (**Figure 2B** and **2C**). To identify major cordycepin-regulated proteins using GO analysis, IPA was used to query 33 proteins that were up- or downregulated by cordycepin, yielding a distinct interconnected network of 27 proteins (**Figure 2D**). Among these, downregulation of ERK/Slug was the center of apoptosis-related protein network.

A549 cells were sensitive to treatment with cordycepin, leading to bax-mediated apoptosis. Cordycepin also inhibits the production of NO by downregulation of iNOS and Cyclooxygenase-2 (COX-2) genes via the suppression of NF-κB activation, Protein kinase B (Akt), and p38 phosphorylation [18]. However, the role of NO-ERK-Slug signaling in the induction of apoptosis remains unclear. Although treatment with L-NAME alone inhibited the production of NO, the treatment in the presence of excess amount of LPS restored NO production (**Figure 4A**). Thereafter, the effect of LPS on cordycepin-induced inhibition of NO production was analyzed. Treatment of A549 cells with cordycepin in the presence of an excess amount of LPS blocked LPS-stimulated production of NO. Western blot analysis revealed that cordycepin-induced reduction in the production NO is associated with an inhibitory effect of cordycepin on NOS in A549 cells. The treatment of cordycepin resulted in the inhibition of iNOS expression in LPS-stimulated A549 cells (**Figure 4B** and **4C**). These observations suggest that cordycepin inhibits the production of NO by inhibiting NOS in A549 cells. Several inflammatory cytokines and chemokines, such as TNF-α, IL-6, TGF-β, and IL-10, have been observed to engage in the initiation, promotion and progression of cancer [20] and are potent inducers of a number of different genes, such as NF-kappaB (NF-κB), p38, signal transducer and activator of transcription 1 (STAT1), and iNOS [19]. LPS stimulates the expression of proinflammatory cytokines and chemokines in classical immune tissues as well as in the skeletal muscle [20]. In this study, LPS-mediated upregulation of the expression and secretion of cytokines and chemokines, such as IL-1β, IL-6, IL-8, CCL5, and TNF-α was observed (**Figure 4D**). These findings indicate towards the correlation between NO and cancer progression upon induction of inflammatory response.

In the present study, the involvement of NO/ERK/Slug signaling pathway in mediating apoptosis in A549 cell line after cordycepin treatment was observed. First, it was found that cordycepin mediated downregulation of ERK phosphorylation by inhibiting the production of NO production, which preceded apoptosis in A549 lung cancer cells. Second, downregulation of p-ERK reduced the expression of Slug protein. Third, cordycepin-mediated inhibition of ERK downregulated the expression of Slug proteins through the activation of GS-

K3β. Finally, siRNA-mediated inhibition of Slug led to upregulation of the levels of pro-apoptotic proteins, such as Bax and cleaved caspase-3.

Previous studies have identified NO as a molecule of interest in carcinogenesis and tumor growth progression. However, there is a considerable controversy, confusion, and debate in understanding its role in tumor biology. It is said to have both, tumoricidal as well as cancer-promoting effects, which rely on its timing, location, and concentration of exposure. NO has been suggested to modulate different cancer-related events, such as angiogenesis, apoptosis, cell cycle, invasion, and metastasis [1]. Previous studies have shown that as the NO levels decrease, a reduction of ERK phosphorylation occurs. On the contrary, increase in NO levels also stimulates ERK activation [21, 22]. NO inhibits the phosphorylation of ERK and promotes cancer cells apoptosis [23]. A reduction in the level of NO by L-NAME and cordycepin led to a decrease in ERK phosphorylation, whereas increase in the levels of NO by LPS resulted in activation of ERK (**Figure 5A** and **5B**). Cordycepin significantly decreased LPS-induced ERK phosphorylation (**Figure 5A**), suggesting that ERK activation is inhibited by inhibition of NO production. A549 cells were also treated with specific NOS inhibitor, L-NAME, at the basal concentration of p-ERK. A dose-dependent reduction in Slug expression was observed (**Figure 5C** and **5D**), further suggesting that cordycepin inhibits NO-mediated ERK and Slug activation.

Slug is regulated by the ERK-Fos-related antigen 1 (Fra-1)/c-Jun signaling axis through the Activator protein 1 (AP1) consensus sequence in the Slug promoter. ERK signaling pathway also facilitates breast cancer cell migration by regulating Slug expression [24]. Slug (SNAI2, Snail2) induces the epithelial mesenchymal transition (EMT) in physiological as well as in pathological contexts. It is implicated in the development and progression of lung cancer [25, 26]. Knockdown of Slug significantly suppressed lung cancer cell proliferation. Furthermore, knockdown of Slug significantly inhibited lung cancer cell invasion and metastasis [27]. We found that cordycepin attenuated p-ERK and Slug, whereas ERK overexpression up-regulated p-ERK and Slug in cordycepin treated A549 cells (**Figure 6A** and **6B**), indicating that cordycepin-mediated ERK inactivation down-regulated the Slug. Also we found siRNA mediated Slug inhibition blocked Slug and enhanced Bax and caspase-3 activation, suggesting that cordycepin-mediated ERK inactivation down-regulated the Slug, leading to the up-regulation of Bax.

Further, effect of ERK induced phosphorylation of GSK3β on cordycepin-mediated inactivation of GSK3β and upregulation of Slug was investigated. In previous studies, it has been demonstrated that ERK associates with and primes GSK3β for its inactivation [28], and that functional regulation of Slug/Snail2 is dependent on GSK3β-mediated phosphorylation [29]. GSK3β regulates EMT and cancer metastasis by degradation of Slug [30]. In the present study, treatment with GSK3β inhibitor LiCl (50 μM) alone increased p-GSK3β and Slug levels (**Figure 6C** and **6D**), whereas cordycepin-mediated inhibition of ERK in A549 cells treated with LPS resulted in decreased p-GSK3β and Slug levels (**Figure 6E** and **6F**). These results indicate that cordycepin-mediated inhibition of ERK downregulates Slug expression through the activation of GSK3β.

In conclusion, it was demonstrated that the levels of Bax protein were dramatically increased by the negative regulation of NO-mediated ERK/Slug expression through the activation of GSK3β in cordycepin-treated A549 cells. These findings provide novel insights into the molecular mechanisms of apoptosis in A549 cell line. Controlling NO expression may, therefore, provide new approaches and strategies to promote apoptosis of A549 cells. Taken together, these results indicate that cordycepin mediates apoptotic regulation of ERK/Slug by Bax through the activation of GSK3β by down-regulating NO. The study also highlighted a potential therapeutic use of cordycepin in the treatment of lung cancer.

Acknowledgements

This research was supported by the Chung-Ang University Research Scholarship Grants in 2016 and Korea Institute of Oriental Medicine (K16060).

Disclosure of conflict of interest

None.

Address correspondence to: Jae-Hong Ko, Department of Physiology, Chung-Ang University, College of Medicine, 84, Heukseok-ro, Dongjak-gu, Seoul 06974, Republic of Korea. Tel: +82-2-820-5647; Fax: +82-2-817-7115; E-mail: akdongyi01@cau.ac.kr; Ik-Soon Jang, Division of Bioconvergence Analysis, Korea Basic Science Institute, Gwahangno 113, Yuseong-gu, Daejeon 305-333, Republic of Korea. Tel: +82-865-3430; Fax: +82-865-3419; E-mail: jangiksn@kbsi.re.kr

References

[1] Choudhari SK, Chaudhary M, Bagde S, Gadbail AR and Joshi V. Nitric oxide and cancer: a review. World J Surg Oncol 2013; 11: 118.

[2] Ying L and Hofseth LJ. An emerging role for endothelial nitric oxide synthase in chronic inflammation and cancer. Cancer Res 2007; 67: 1407-1410.

[3] Hickok JR and Thomas DD. Nitric oxide and cancer therapy: the emperor has NO clothes. Curr Pharm Des 2010; 16: 381-391.

[4] Wagner EF and Nebreda AR. Signal integration by JNK and p38 MAPK pathways in cancer development. Nat Rev Cancer 2009; 9: 537-549.

[5] Fremin C and Meloche S. From basic research to clinical development of MEK1/2 inhibitors for cancer therapy. J Hematol Oncol 2010; 3: 8.

[6] McCain J. The MAPK (ERK) pathway: investigational combinations for the treatment of BRAF-mutated metastatic melanoma. P T 2013; 38: 96-108.

[7] Kohno M and Pouyssegur J. Targeting the ERK signaling pathway in cancer therapy. Ann Med 2006; 38: 200-211.

[8] Shih JY and Yang PC. The EMT regulator slug and lung carcinogenesis. Carcinogenesis 2011; 32: 1299-1304.

[9] Martin TA, Goyal A, Watkins G and Jiang WG. Expression of the transcription factors snail, slug, and twist and their clinical significance in human breast cancer. Ann Surg Oncol 2005; 12: 488-496.

[10] Catalano A, Rodilossi S, Rippo MR, Caprari P and Procopio A. Induction of stem cell factor/c-Kit/slug signal transduction in multidrug-resistant malignant mesothelioma cells. J Biol Chem 2004; 279: 46706-46714.

[11] Barrallo-Gimeno A and Nieto MA. The snail genes as inducers of cell movement and survival: implications in development and cancer. Development 2005; 132: 3151-3161.

[12] Cha HS, Bae EK, Ahn JK, Lee J, Ahn KS and Koh EM. Slug suppression induces apoptosis via Puma transactivation in rheumatoid arthritis fibroblast-like synoviocytes treated with hydrogen peroxide. Exp Mol Med 2010; 42: 428-436.

[13] Yin JQ, Shen JN, Su WW, Wang J, Huang G, Jin S, Guo QC, Zou CY, Li HM and Li FB. Bufalin induces apoptosis in human osteosarcoma U-2OS and U-2OS methotrexate300-resistant cell lines. Acta Pharmacol Sin 2007; 28: 712-720.

[14] Jeong JW, Jin CY, Park C, Hong SH, Kim GY, Jeong YK, Lee JD, Yoo YH and Choi YH. Induction of apoptosis by cordycepin via reactive oxygen species generation in human leukemia cells. Toxicol In Vitro 2011; 25: 817-824.

[15] Pan BS, Wang YK, Lai MS, Mu YF and Huang BM. Cordycepin induced MA-10 mouse Leydig tumor cell apoptosis by regulating p38 MAPKs and PI3K/AKT signaling pathways. Sci Rep 2015; 5: 13372.

[16] Mehta RG, Murillo G, Naithani R and Peng X. Cancer chemoprevention by natural products: how far have we come? Pharm Res 2010; 27: 950-961.

[17] Jin S, Shen JN, Wang J, Huang G and Zhou JG. Oridonin induced apoptosis through Akt and MAPKs signaling pathways in human osteosarcoma cells. Cancer Biol Ther 2007; 6: 261-268.

[18] Kim HG, Shrestha B, Lim SY, Yoon DH, Chang WC, Shin DJ, Han SK, Park SM, Park JH, Park HI, Sung JM, Jang Y, Chung N, Hwang KC and Kim TW. Cordycepin inhibits lipopolysaccharide-induced inflammation by the suppression of NF-kappaB through Akt and p38 inhibition in RAW 264.7 macrophage cells. Eur J Pharmacol 2006; 545: 192-199.

[19] Landskron G, De la Fuente M, Thuwajit P, Thuwajit C and Hermoso MA. Chronic inflammation and cytokines in the tumor microenvironment. J Immunol Res 2014; 2014: 149185.

[20] Frost RA, Nystrom GJ and Lang CH. Lipopolysaccharide regulates proinflammatory cytokine expression in mouse myoblasts and skeletal muscle. Am J Physiol Regul Integr Comp Physiol 2002; 283: R698-709.

[21] Castellano I, Ercolesi E and Palumbo A. Nitric oxide affects ERK signaling through down-regulation of MAP kinase phosphatase levels during larval development of the ascidian Ciona intestinalis. PLoS One 2014; 9: e102907.

[22] Song JS, Kang CM, Yoo MB, Kim SJ, Yoon HK, Kim YK, Kim KH, Moon HS and Park SH. Nitric oxide induces MUC5AC mucin in respiratory epithelial cells through PKC and ERK dependent pathways. Respir Res 2007; 8: 28.

[23] Feng X, Sun T, Bei Y, Ding S, Zheng W, Lu Y and Shen P. S-nitrosylation of ERK inhibits ERK phosphorylation and induces apoptosis. Sci Rep 2013; 3: 1814.

[24] Chen H, Zhu G, Li Y, Padia RN, Dong Z, Pan ZK, Liu K, Huang S. Extracellular signal-regulated kinase signaling pathway regulates breast cancer cell migration by maintaining slug expression. Cancer Res 2009; 69: 9228-9235.

[25] Tanno B, Sesti F, Cesi V, Bossi G, Ferrari-Amorotti G, Bussolari R, Tirindelli D, Calabretta B, Raschellà G. Expression of Slug is regulated by c-Myb and is required for invasion and bone marrow homing of cancer cells of different origin. J Biol Chem 2010; 285: 29434-45.

[26] Larue L, Bellacosa A. Epithelial-mesenchymal transition in development and cancer: role of phosphatidylinositol 3' kinase/AKT pathways. Oncogene 2005; 24: 7443-54.

[27] Wang YP, Wang MZ, Luo YR, Shen Y, Wei ZX. Lentivirus-mediated shRNA interference targeting SLUG inhibits lung cancer growth and metastasis. Asian Pac J Cancer Prev 2012; 13: 4947-4951.

[28] Ding Q, Xia W, Liu JC, Yang JY, Lee DF, Xia J, Bartholomeusz G, Li Y, Pan Y, Li Z, Bargou RC, Qin J, Lai CC, Tsai FJ, Tsai CH and Hung MC. Erk associates with and primes GSK-3beta for its inactivation resulting in upregulation of beta-catenin. Mol Cell 2005; 19: 159-170.

[29] Kim JY, Kim YM, Yang CH, Cho SK, Lee JW and Cho M. Functional regulation of Slug/Snail2 is dependent on GSK-3beta-mediated phosphorylation. FEBS J 2012; 279: 2929-2939.

[30] Kao SH, Wang WL, Chen CY, Chang YL, Wu YY, Wang YT, Wang SP, Nesvizhskii AI, Chen YJ, Hong TM and Yang PC. GSK3beta controls epithelial-mesenchymal transition and tumor metastasis by CHIP-mediated degradation of Slug. Oncogene 2014; 33: 3172-3182.